ISSN 2075-1087, Gyroscopy and Navigation, 2022, Vol. 13, No. 4, pp. 189–209. © Pleiades Publishing, Ltd., 2022.
Russian Text © The Author(s), 2022, published in Giroskopiya i Navigatsiya, 2022, No. 4, pp. 3–35.

State-of-the-Art Strapdown Airborne Gravimeters: Analysis of the Development

V. G. Peshekhonov[a, b], O. A. Stepanov[a, b, *], V. G. Rozentsvein[a], A. A. Krasnov[a, b, **], and A. V. Sokolov[a, b]

[a] *Concern CSRI Elektropribor, JSC, St. Petersburg, Russia*

[b] *ITMO University, St. Petersburg, Russia*

**e-mail: soalax@mail.ru*

***e-mail: anton-krasnov@mail.ru*

Received November 25, 2022; revised December 27, 2022; accepted December 28, 2022

Abstract—The paper analyzes the development of strapdown inertial airborne gravimeters, which have significant advantages over gyrostabilized gravimeters in terms of size, power consumption and cost and substantially expand the capabilities of gravity survey. Technical solutions are described that make implementation of strapdown airborne gravimeters possible. The trends in their development are discussed, including integration of data from strapdown and gyrostabilized gravimeters.

Keywords: Earth's gravitational field, gravity disturbance vector, gravity anomaly, strapdown airborne gravimeter, vector airborne gravimeter, scalar airborne gravimeter, inertial measurement unit, global navigation satellite systems

DOI: 10.1134/S2075108722040101

INTRODUCTION

Knowledge of the Earth's gravitational field (EGF) is necessary for a variety of problems that researchers face in geodesy, geology, and high-precision inertial navigation. The methods used to study the EGF differ in accuracy and spatial resolution; among them are the following: ground-based gravity survey at certain points on the Earth's surface, marine and airborne gravity survey from vehicles, and satellite methods (space geodesy) [1–12].

Ground-based gravity survey is the most accurate of them; it has the best spatial resolution, but a very low productivity [9, 12], which makes it inefficient to carry out expeditionary fieldwork over large areas. Besides, not all areas on Earth are accessible for such surveys.

The methods of space geodesy make a significant contribution to the creation and development of global EGF models [6, 10]. However, the EGF is weaker at high altitudes, which limits their spatial resolution; therefore, it is possible to obtain accurate information only about the long-wave part of the field and does not allow local field anomalies to be determined with sufficient resolution only from satellite information [8, 10, 13].

Currently, survey from moving vehicles is the most important link between ground survey and satellite methods in terms of accuracy and spatial resolution.

The main objective of gravimetry is to determine the anomalous EGF characterized by the gravity disturbance vector (GDV), which is defined as the difference between the gravity vector and the normal gravity vector at the same measurement point. A special case of this problem is determination of the gravity anomaly (GA), which is the GDV magnitude along the true vertical [7, 9, 10].

Since this paper is largely devoted to the issues related to inertial gravimetry, let us elucidate the meaning of this term. In so doing, it makes sense to start from the definition of gravimetry as a science, as is done in most cases, for example, in [5, 10, 14, 15]. Thus, inertial gravimetry should be understood as a science, which is a particular branch of gravimetry. Note that this aspect is often overlooked and inertial gravimetry is introduced as a method for determining the EGF, as a technology, etc. In our opinion, such terminological ambiguity can be found in V. Torge [5] and in the works of the famous Canadian scientist K.R. Schwartz [16], who, actually, laid the foundations of the modern theory of inertial gravimetry [16, 17]. In Russia, the first publications on inertial gravimetry belong to V.L. Panteleev and his colleagues [18, 19], in which, though oddly enough, the definition of inertial gravimetry is not explicitly introduced. Although in one of his latest works Panteleev suggests using the term 'inertial gravimetry' to refer to all problems arising in the measurement of the gravitational field intensity in motion [20]. In the works on this subject published by Russian scientists later, inertial gravimetry is defined quite broadly as the applied science of determining the gravity force from the motion of a proof mass [15]. In view of the above, in this paper, the term *inertial gravimetry* is used in reference to a branch of gravimetry concerned with the study (measurement) of EGF on a moving platform by means of inertial technologies. Accordingly, gravimeters designed to determine the anomalous EGF on a moving platform, built with the use of the same technologies, are called inertial gravimeters.

Three types of measuring instruments can be used to solve the problems faced by inertial gravimetry: inertial scalar gravimeters, inertial vector gravimeters, and gravity gradiometers.

Inertial scalar gravimeters, or simply scalar gravimeters, are designed to determine the GDV magnitude along the true vertical. Modern scalar gravimeters for vehicles are mainly based on technologies that use gyrostabilized platforms and data from global navigation satellite systems (GNSS). These technologies are supported by advanced hardware and software and provide high accuracy of GA measurement—0.05–0.5 mGal, which makes it possible to meet various challenges of gravimetry [10]. However, gravimeters using gyrostabilized platforms have a number of drawbacks, the main of which are the following [9, 21, 22]:

• large weight and dimension characteristics – volume up to 100 L, weight up to 100 kg;

• significant power consumption, reaching hundreds of watts;

• high cost due to the presence of a gyrostabilized platform in particular;

• the need to maintain gravimeters during operation;

• high cost of expeditionary fieldwork because of the operating cost of vehicles—surface vessels and aircraft;

• difficulties of using unmanned aerial vehicles (UAVs) as carriers, difficulties in conducting drape surveys.

Scalar gravimeters for vehicles based on technologies that make use of strapdown inertial systems do not have such drawbacks. They are called strapdown inertial scalar gravimeters, or simply strapdown scalar gravimeters [9].

Inertial vector gravimeters are designed to determine all three components of the GDV, the estimates of which refer to the coordinate frame associated with the reference ellipsoid. As with scalar gravimeters, vector gravimeters can be based on the use of either platform inertial systems or strapdown systems. In the latter case, they are also called strapdown inertial vector gravimeters, or simply strapdown vector gravimeters [9, 10, 19].

Strapdown vector gravimeters, like scalar ones, are free from the shortcomings inherent in gyrostabilized gravimeters. In addition, they have significant advantages over scalar ones in terms of determining the EGF parameters. This is due to the fundamental possibility of calculating deflections of the vertical (DOV) and geoid heights along the motion path directly from their readings [21, 23–25]. This is much simpler to implement and much less laborious compared to finding such parameters using gravity anomalies over a large area, as required by the Vening Meinesz and Stokes formulas [5]. In addition, independent measurements of the horizontal components of the gravity make the solution of the inverse problem of geophysics simpler. The area survey data of the GDV components allow gravity gradients to be calculated with a minimum amount of data that make it possible to detect drastic changes in the density of the Earth's crust structure [26, 27].

Gravity gradiometers are designed to determine the components of the tensor of the geopotential second-order derivatives [10, 28]. The advantage of using geopotential second-order derivatives is the possibility of obtaining high-resolution increments of the full gravity vector, GDV, and DOV. However, the development, manufacturing and operation of gravity gradiometers are among the most sophisticated technologies of modern instrument engineering. Despite the impressive results in gravity exploration and creation of global EGF models based on the data from satellite missions, gravity gradiometry remains a unique and expensive method for determining EGF parameters [29–33].

From the foregoing it follows that creation of strapdown inertial scalar and vector gravimeters is highly relevant since they will allow improving the accuracy and spatial resolution of the EGF parameter surveying.

Airborne gravity survey has obvious advantages, such as high efficiency and the ability to perform measurements in hard-to-reach areas, which stimulates its active development [9, 11, 15, 21, 34–37]. At the same time, it has a number of specific features [5]:

• high speed and altitude of the aircraft limit the spatial resolution of measurements;

• a wide range of disturbing accelerations caused by aircraft motion imposes increased requirements on the accuracy of the navigation support needed, in particular, to compensate for accelerations in gravimeter readings, including calculation of the Eötvös correction taking into account the Earth's compression and flight altitude [5, 38];

• the need to reduce the obtained estimates from the flight altitude to the ellipsoid surface.

Note that the first feature is less specific to helicopters and various kinds of UAVs.

This paper is devoted to the problems associated with the creation of strapdown inertial airborne gravimeters and prospects for their development, with the emphasis on the hardware of airborne gravimeters and the currently attainable measurement accuracies. However, it should be noted that in strapdown inertial airborne gravimeters, a significant role belongs to the methods for processing measurement information obtained during the gravity survey [10]. A detailed discussion of data processing methods is beyond the scope of this paper since it deserves special consideration.

The paper consists of four sections. Section 1 considers the operation principles of strapdown inertial scalar and vector gravimeters based on the data integration of strapdown systems and GNSS. Section 2 briefly describes the history of the creation and development of strapdown inertial airborne gravimeters and introduces the leading companies involved in their creation. Section 3 is devoted to airborne gravimeters which are currently either in trial operation or have undergone full-scale tests. Section 4 discusses the trends in the development of strapdown inertial airborne gravimeters. Finally, the main conclusions are made based on the results of the review.

1. BASIC RELATIONS AND PRINCIPLE OF OPERATION OF STRAPDOWN GRAVIMETERS

To explain the principle of operation of strapdown gravimeters, let us discuss the main mathematical relations used to describe its operation. This will require the following four right orthogonal reference frames: the Earth-Centered Inertial (ECI) frame (*i*-frame), the Earth-Centered Earth-Fixed (ECEF) frame (*e*-frame), the body-fixed frame (*b*-frame)—the frame associated with the vehicle, and the local navigation frame (*n*-frame) [39, 40]. Assume that the sensitive masses of a triad of accelerometers are pointlike and coincide at a single point determined in the inertial frame by the radius vector *r*. The *b*-frame and the *n*-frame are assumed to have a common origin at this point. In the *b*-frame, one of the axes *x* is directed parallel to the diametrical plane of the vehicle (along the vehicle), the second one, *y*, is pointing to the right, and the third one, *z*,—downward; in the *n*-frame, one of the axes *N* is pointing to the north, the second one, *E*, to the east, and the third one, *D*, is set by the inner normal to the Earth ellipsoid or reference ellipsoid [39].

As noted in [10], like in the case of strapdown inertial navigation systems (SINS), the equations for the ideal operation of a strapdown vector gravimeter can be written using different reference frames. For definiteness, here we will focus on the use of the local navigation frame.

Let us write the readings of the accelerometers that measure specific force *f*, which is the difference between the absolute acceleration of the accelerometer proof mass, due to the vehicle motion, and the gravity force *g* [9, 35]:

$$f^i = \ddot{r}^i - g^i. \tag{1}$$

In what follows, the superscript is used to designate the coordinate frame in which the corresponding vector is specified. Absolute acceleration is also called inertial or kinematic acceleration [41–43].

From Equation (1) we derive the following formula for the gravity vector:

$$g^i = \ddot{r}^i - f^i. \tag{2}$$

Assume that the gravity vector must be determined in *n*-frame. In this case, accelerometer measurements from the *b*-frame must be transformed to the *n*-frame, for which purpose we use the direction cosine matrix C_b^n defined as [39, 44, 45]:

$$C_b^n = \begin{bmatrix} \cos\theta\cos\psi & -\cos\chi\sin\psi + \sin\chi\sin\theta\cos\psi & \sin\chi\sin\psi + \cos\chi\sin\theta\cos\psi \\ \cos\theta\sin\psi & \sin\chi\sin\theta\sin\psi + \cos\chi\cos\psi & -\sin\chi\cos\psi + \cos\chi\sin\theta\sin\psi \\ -\sin\theta & \sin\chi\cos\theta & \cos\chi\cos\theta \end{bmatrix}, \tag{3}$$

where ψ, θ, χ are, respectively, the angles of rotation about the axes of yaw (vertical axis directed downward), pitch (axis pointing to the right), and roll (axis directed along the vehicle) of the *b*-frame.

In order to take into account the Coriolis acceleration and centrifugal forces in the accelerometer readings, it is necessary to introduce the Eötvös correction δg^n_{eot} into the equation $\delta g^n = g^n - \gamma^n$ that defines the GDV:

$$\delta g^n = \ddot{r}^n - C_b^n f^b + \delta g^n_{eot} - \gamma^n, \tag{4}$$

where $\gamma^n = [0\ \ 0\ \ \gamma_D]^T$ is the vector of normal gravity at a height *h* above the ellipsoid, directed along its normal.

Clairaut's equation can be used to calculate the values of γ_D, taking into account the vertical gradient of the normal gravity [1]:

$$\gamma_D = \gamma_e(1 + \beta\sin^2\varphi - \beta_1\sin^2 2\varphi) - 2\omega_0^2 h, \tag{5}$$

in which $\beta = \dfrac{\gamma_p - \gamma_e}{\gamma_e}$ is the relative excess of gravity at the pole; $\alpha = \dfrac{a-b}{a}$ is ellipsoid flattening; a and b are the major and minor semiaxes of the ellipsoid; $\beta_1 = \dfrac{\alpha^2}{8} + \dfrac{1}{4}\alpha\beta$; γ_p, γ_e are normal gravities at the pole and equator, respectively; ω_0 is the Schuler frequency (1.24×10^{-3} s^{-1}); h is the vehicle height above the ellipsoid.

The Eötvös correction is given as [2, 41]:

$$\delta g^n_{eot} = 2\Omega^n_{ie}\dot{r}^n + \Omega^n_{en}\dot{r}^n, \tag{6}$$

where

$$\Omega^n_{ie} = \omega_{ie}\begin{bmatrix} 0 & \sin\varphi & 0 \\ -\sin\varphi & 0 & -\cos\varphi \\ 0 & \cos\varphi & 0 \end{bmatrix} \tag{7}$$

is a skew-symmetric matrix that determines the ECI frame rotation relative to the inertial one, specified in the n-frame (hereinafter, the first subscript refers to the frame relative to which the coordinate frame determined by the second subscript rotates. The superscript refers to the frame in which this rotation is set); ω_{ie} is the Earth's angular velocity; φ is the geodetic latitude;

$$\Omega^n_{en} = \begin{bmatrix} 0 & \dfrac{\dot{r}_E\tan\varphi}{R_E + h} & -\dfrac{\dot{r}_N}{R_N + h} \\ -\dfrac{\dot{r}_E\tan\varphi}{R_E + h} & 0 & -\dfrac{\dot{r}_E}{R_E + h} \\ \dfrac{\dot{r}_N}{R_N + h} & \dfrac{\dot{r}_E}{R_E + h} & 0 \end{bmatrix} \tag{8}$$

is a skew-symmetric matrix that determines the translational speed of rotation of the n-frame relative to the e-frame; $\dot{r}_N, \dot{r}_E, \dot{r}_D$ are projections of the carrier velocity on the axes of the local navigation frame (N – northern, E – eastern, and D – vertical); R_N and R_E are the ellipsoid radii of curvature in the meridian plane and the first vertical, respectively;

$$\dot{r}^n = \begin{bmatrix} \dot{r}_N \\ \dot{r}_E \\ \dot{r}_D \end{bmatrix} = \begin{bmatrix} (R_N + h)\dot{\varphi} \\ (R_E + h)\cos\varphi\dot{\lambda} \\ -\dot{h} \end{bmatrix}, \tag{9}$$

where λ is the geodetic longitude. In what follows, the superscript of the vector components is omitted for simplicity.

The first term of Eq. (6) defines the Coriolis acceleration; the second is centrifugal acceleration due to the vehicle motion relative to the Earth. The above assumes that the centrifugal acceleration due to the Earth's rotation is already included in γ^n.

The direction cosine matrix C^n_b can be determined by integrating the Poisson equation given as [44]:

$$\dot{C}^n_b = C^n_b\Omega^b_{ib} - \Omega^n_{in}C^n_b, \tag{10}$$

where

$$\Omega^b_{ib} = \begin{bmatrix} 0 & -\omega^b_z & \omega^b_y \\ \omega^b_z & 0 & -\omega^b_x \\ -\omega^b_y & \omega^b_x & 0 \end{bmatrix} \tag{11}$$

is a skew-symmetric matrix that determines the b-frame rotation relative to the i-frame in the b-frame axes according to the measurements ω^b_x, ω^b_y, ω^b_z from the angular rate sensors (ARS);

$$\Omega^n_{in} = \begin{bmatrix} 0 & \omega_{ie}\sin\varphi + \dfrac{\dot{r}_E\tan\varphi}{R_E + h} & -\dfrac{\dot{r}_N}{R_N + h} \\ -\omega_{ie}\sin\varphi - \dfrac{\dot{r}_E\tan\varphi}{R_E + h} & 0 & -\omega_{ie}\cos\varphi - \dfrac{\dot{r}_E}{R_E + h} \\ \dfrac{\dot{r}_N}{R_N + h} & \omega_{ie}\cos\varphi + \dfrac{\dot{r}_E}{R_E + h} & 0 \end{bmatrix} \tag{12}$$

is a skew-symmetric matrix that defines the rotation of the n-frame relative to the i-frame in the axes of the n-frame.

The GDV is determined from Eqs. (4) and (6), so that we can write the following equation:

$$\delta g^n = \ddot{r}^n - C^n_b f^b + (2\Omega^n_{ie} + \Omega^n_{en})\dot{r}^n - \gamma^n. \tag{13}$$

Equation (13) defines both the horizontal and vertical components of the GDV. For the vertical component, it is easy to derive the following equation from (13):

$$\delta g_D = \ddot{r}_D - f_D + \left(2\omega_{ie}\cos\varphi + \frac{\dot{r}_E}{R_E + h}\right)\dot{r}_E + \frac{\dot{r}_N^2}{R_N + h} - \gamma_D. \tag{14}$$

Taking into consideration the above relations, it is possible to explain the principle of operation of the strapdown vector gravimeter (Fig. 1), the input information for which is the data from the inertial measurement unit (IMU) and GNSS.

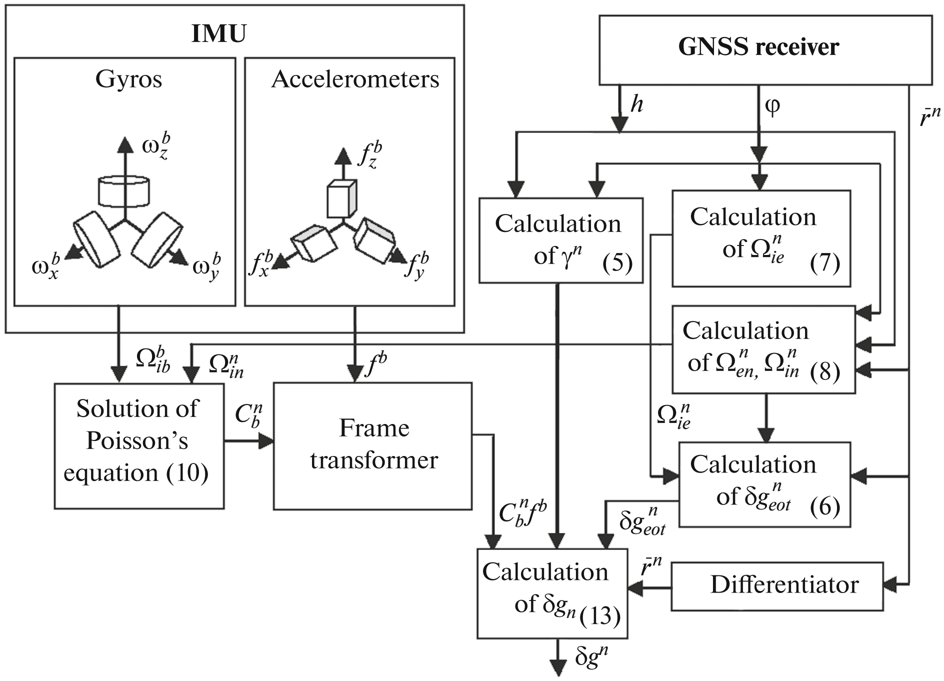

Fig. 1. Block diagram of a strapdown inertial vector gravimeter.

A triad of accelerometers in the body-fixed frame measures three components f_x^b, f_y^b, f_z^b of vector f^b of the specific force. A triad of ARS measures three components $\omega_x^b, \omega_y^b, \omega_z^b$ of the vehicle's angular velocity vector in inertial space. They determine matrix Ω_{ib}^b. Next, the specific force vector f^b is converted from the body-fixed frame to the local navigation frame using the direction cosine matrix C_b^n. This matrix can be calculated by solving Poisson's equation using the data on the vehicle angular velocity Ω_{ib}^b obtained from the ARS and the angular rate of rotation of the local navigation frame Ω_{in}^n. The GNSS receiver generates geodetic coordinates and the vehicle velocity components, which are used to calculate Eötvös correction, the normal gravity vector γ^n, matrices $\Omega_{ie}^n, \Omega_{en}^n, \Omega_{in}^n$ and $\ddot{r}^n$. Further, Eqs. (13) or (14) are used to determine either all components of the GDV δg^n or GA δg_D.

From the above description it follows that the strapdown vector gravimeter includes

• a triad of accelerometers to measure three components of the specific force f_x^b, f_y^b, f_z^b in the body-fixed frame;

• a triad of gyroscopic ARS to measure three components of the angular rate of rotation of the local navigation frame relative to the inertial space in the body-fixed frame;

• high-precision GNSS receiver to determine pseudo-ranges and pseudo-velocities needed to generate the motion parameters of the vehicle, i.e. geodetic coordinates and components of velocities in the local navigation frame;

• a computer in particular to determine the transformation matrix C_b^n from the body-fixed frame to the local navigation frame and the Eötvös correction.

The description of the operating principle of the strapdown inertial vector gravimeter is given on the assumption that all input data are measured without errors. Since this condition is not feasible, the methods for processing measurement information obtained as a result of gravity survey are of great importance.

As noted in the introduction, the issues related to the processing of measurement information in strapdown airborne gravimeters are beyond the scope of this work. Note only that strapdown onboard gravimetry uses a variety of data processing methods that can be conditionally divided into two groups [41, 46]. In the so-called *direct* methods, the GDV is determined by forming the difference between absolute accelerations and specific forces measured by accelerometers. In this case, GNSS data are used to determine $\ddot{r}^n$ [9, 35, 41, 47, 48]. In fact, the block diagram shown in Fig. 1 fits this group. In *indirect* methods, when determining the GDV, it is not accelerations that are compared, but position and (or) velocity measurements obtained from GNSS data and inertial sensors, which explains the name of the method [41, 47–50]. Algorithms based on the use of the Kalman filter have received the greatest application here. The specificity of particular variants for designing such processing algorithms depends on the structure of the state vector and the rules for the formation of measurements used in the Kalman filter. For example, they can be differences in coordinates and (or) velocities obtained from GNSS data and inertial sensors, the so-called loosely coupled integration. In some cases, preference is given to a tightly coupled integration, in which differences between the measured and calculated values of pseudoranges and (or) pseudovelocities are used as measurements in the Kalman filter [10, 51–53]. Processing of measurement information in strapdown inertial gravimeters involves various kinds of additional information, using special algorithms for filtering and smoothing of intermediate and measurement information in online or offline modes, special algorithms for calibration and compensation for systematic errors of inertial sensors, various mathematical error models of the sensors used and models of the estimated GA. An important role belongs to the algorithms for obtaining high-accuracy information based on GNSS data and the ways of how the problem of synchronization of inertial and GNSS data is solved [10].

It follows from the foregoing that a strapdown inertial gravimeter is basically a sophisticated measuring system that includes inertial, satellite and computational parts as its hardware, while the algorithmic part provides the necessary calculations both on board the vehicle and in the postprocessing mode. It is easy to see that the strapdown inertial gravimetric system has the same composition as the SINS integrated with GNSS. By analogy with SINS, we can introduce the corresponding abbreviation SIGS.

A special feature of SIGS lies in the compulsory provision of high-accuracy external information about the vehicle's coordinates and speed, which makes it possible to simplify the ideal operation algorithms in comparison with those used in SINS [10]. In particular, we can distinguish two separate tasks—determining the horizontal components of the GDV and determining the GA—by analogy with how a vertical channel is allocated in SINS. Note that both SIGS and SINS require initial information about the vehicle orientation. It should be emphasized that in a SIGS, the inertial system is not required to function as a navigation system, but can only be considered as a recorder of measurements of inertial sensors, such as accelerometers, gyroscopic ARS synchronized with GNSS data [10]. At the same time, it should be borne in mind that in contrast to SINS integrated with GNSS, simplification of SIGS algorithms results in its inability to determine navigation parameters when the GNSS data become degraded or unavailable.

The principle of operation of the strapdown vector gravimeter is described above; however, it is clear that the vector gravimetry problem can also be solved with the use of platform systems. If the navigation frame is represented by the local navigation frame, there is no need to transform specific forces measured by accelerometers from the body-fixed frame to the local navigation frame [10].

And one more remark. The above described principle of operation of the inertial vector gravimeters was considered without reference to the type of the vehicle—aircraft or marine vessel. Nowadays, strapdown airborne gravimeters, to which this paper is devoted, have received widest recognition and are being actively developed. At the same time, vector gravimeters can also be used on marine vessels, although they have their own specificity. It is known that when measuring GA onboard marine vessels, acceptable accuracies can be achieved without high-accuracy external information needed to compensate for inertial accelerations [54]. Note that the inertial-geodetic method used to determine horizontal components of the GDV [10] can essentially be considered as a variant of the vector gravimeter intended to determine these components of the GDV. In this connection, it might be well to point out that questions of SIGS design for marine vessels require special consideration.

2. BRIEF HISTORY OF THE CREATION AND DEVELOPMENT OF STRAPDOWN AIRBORNE GRAVIMETERS

As noted in a number of publications [11, 15, 55], proposals for the construction of airborne inertial scalar gravimeters appeared in the late 1950s and early 1960s [56, 57]. The first tests with an airborne LaCoste & Romberg (LCR) sea gravimeter were carried out on November 6 and 7, 1958, on board a US Air Force KC-135 aircraft over Edwards Air Force Base in California. 5-minute average gravity readings were obtained with an accuracy of better than 10 mGal [57]. In 1959–1960, in-flight experiments began with heavily damped quartz string gravimeters (USSR) and the LCR marine gravimeter (USA) mounted in gimbal suspensions. Since the instruments of those times did not have the required accuracy, the purpose of the tests was to study the capabilities of airborne gravimetry. Gravimeters worked in conjunction with photogrammetric cameras and/or Doppler radar systems to determine position and unique hypsometers to measure height. Helicopters were used to improve the accuracy of the measurements, since they move at low speeds and low altitudes. In 1965, tests were carried out on a US Air Force CH-3E helicopter equipped with a gimbaled LCR marine gravimeter. The helicopter location was determined using radar tracking, and the altitude was measured with a laser altimeter.

The main difficulties in airborne gravimetry at that time were caused by inaccuracies in positioning and determination of the aircraft flight altitude. It was owing to the active development of satellite navigation systems in the late 1980s that the main factor restrain-

Table 1. Models of SAGs and their designers

Model	Designer	Year	References
Laseref III	University of Calgary, Canada Honeywell, USA	1995	17, 24, 49, 72–75
LITTON LN-200	Astronomical Observatory of the University of Porto, Portugal Litton, USA	1997	76, 77
SAGEM Sigma 30,	University FAF Munich, Germany SAGEM, France	2003	78
SAGS4	Bavarian Academy of Sciences and Humanities, Munich, Germany	2005	79
SGA-WZ-01 SGA-WZ-02	Laboratory of Inertial Technology, National University of Defense Technology, China	2008	80–84
AIRINS	iXSea, France	2010	48
GT-X	Gravtechology, JSK STC; Ramensky Instrument Engineering Plant; Laboratory of Control and Navigation, Moscow State University, Russia	2011	85
iNAV-RQH	iMAR Navigation gmbH, Reihersbruch, Germany	2013	9, 55, 94, 86–89, 94
iNAT-RQH		2016	
iNAV-FMS		2017	
iCORUS+iDGU-100x			
iCORUS: iCORUS-01* iCORUS-01-wts** iCORUS-02 iCORUS-02-wts iCORUS-03		2020	

* Subject to export restrictions; ** wts—without thermal stabilization.

ing the development of airborne gravimetry was overcome [57–60]. At the same time, numerous works began to appear on various aspects of research, design and testing of strapdown airborne inertial scalar gravimetric systems based on SINS (hereinafter referred to as strapdown airborne gravimeters (SAG).

Already in 1986, based on the results of full-scale tests, it was shown that a SINS IMU can provide an error in determining the vertical components of the gravity vector or the GDV from 2.5 to 4 mGal [61]. The measurements were performed on a ground vehicle using ZUPT (Zero Velocity Update) corrections [9, 62, 63]. This type of correction involves periodic stops (landings) of the vehicle and uses information about its zero speed. It is clear that in airborne gravimetry, corrections of this type can be actively used only when helicopters and UAVs are used as SAG carriers [64, 65].

In recent years, a large volume of airborne gravity surveys has been conducted. At the same time, the SAG hardware has been actively developed in order to increase the accuracy of inertial sensors, improve thermal stabilization systems, reduce weight and dimension characteristics, introduce methods for combining gravimetric sensors of various types, etc. Significant work has also been carried out to improve the efficiency of algorithmic support for both scalar and vector SAGs.

As a rule, SAGs are designed with the use of the hardware of companies that are advanced in their field, such as Honeywell [66], Litton (in 2001, Litton was acquired by Northrop Grumman) [67], SAGEM (in 2005, SAGEM merged with Snecma to form the SAFRAN holding [68], iXSea [69], iMAR [70], Gravtechology JSK STC [71]. Table 1 provides information about the main currently known scalar SAGs and their designers (the authors were unable to find information about any commercially available vector SAGs). Also given are some publications that describe the results obtained with these gravimeters.

3. STRAPDOWN AIRBORNE GRAVIMETERS

This section considers the SAGs which have successfully passed full-scale tests, so that their results served the basis for further development and creation of advanced gravimeters. Some of the SAGs described below are currently in operation.

Table 2. Specifications of laser gyroscopes GG1342 and accelerometers QA2000

Parameter	Gyroscopes	Accelerometers
Bias	0.003 deg/h	10–25 mGal
Scale factor stability	1.0 ppm	25–50 ppm
Misalignment	2 arcsec	5 arcsec
Random noise (σ)	0.001°/√h	5 mGal

3.1. Strapdown Gravimeter Based on the Laseref III (LRF III) INS, Canada

The first prototype of the scalar SAG was developed at the University of Calgary, Canada. It was based on the Honeywell Laseref III (LRF III) INS built on GG1342 laser gyroscopes and QA2000 accelerometers, the characteristics of which are presented in Table 2 [72].

In June 1995, the first SAG in-flight tests were carried out in a highly gravitationally anomalous area over the Rocky Mountains in Canada (GA difference in the range from –70 to 100 mGal). The test program included 4 tacks with a length of about 250 km. The flight speed was 430 km/h, which corresponded to a spatial resolution of 5–7 km with the use of a low-pass filter with a cutoff frequency from 1/90 to 1/120 Hz. The flight altitude above the ellipsoid averaged 5.5 km. To minimize the impact of turbulence, flights were performed from 7 to 11 a.m. [17, 72].

The test results showed that the root-mean-square error (RMSE) of GA determination for an individual tack was 3 mGal at a spatial resolution of 5 km and 2 mGal at a resolution of 7 km. When compared with the ground survey data, the RMSE of the measurement results was 3 mGal for both levels of spatial resolution. The results of the first tests motivated the designers to further research. The results of data processing from the campaign of 1995 are discussed in [24, 50] and the subsequent tests conducted in September 1996, in [72].

In June 1998, the University of Calgary together with Kort & Matrikelstyrelsen (Denmark) (Danish National Survey and Cadastre) conducted an airborne gravity survey off the western coast of Greenland using LRF-III and LCR gravimeters installed onboard the Twin Otter aircraft. Such a comparison of strapdown and gyrostabilized gravimeters was carried out for the first time. Two survey lines were laid over the marine gravity survey area to estimate the accuracy of the airborne gravimeter measurements. The test results showed that after elimination of linear trends, the GA estimates of the two airborne gravimeters, agreed with the marine survey data at a level of 2–3 mGal [73].

Based on the results of those tests, it was concluded that the integration of data from strapdown and gyrostabilized gravimeters was promising in terms of improving the accuracy and spatial resolution of the survey [72–74]. The last tests of the LFR III strapdown gravimeter mentioned in the literature were carried out in 2000 in the vicinity of Ottawa, Canada [75, 76].

3.2. Strapdown Airborne Gravimeter Based on the LITTON LN-200 IMU, Portugal

In 1997, the Astronomical Observatory of the University of Porto (AOUP), Portugal, developed a SAG based on the inexpensive tactical-grade Litton LN-200 IMU. References [76, 77] present the results of an airborne gravity survey in the area of the Azores aimed to refine the geoid model in this region. The vertical component of the gravity vector was estimated with an error of 5–10 mGal at a spatial resolution of 10 km. The results of the in-flight tests of this airborne gravimeter are described in Subsection 4.8, which includes, among other things, a comparison of the results obtained using different gravimeters.

3.3. Strapdown Airborne Gravimeter Based on the SAGEM Sigma 30 INS, Germany

The SAG based on SAGEM Sigma 30 INS was developed in the early 2000s at the University FAF Munich [78]. The INS developed by SAGEM (France) contained triads of ring laser gyroscopes (RLG) and pendulous accelerometers. Satellite data were obtained from the multiantenna equipment (Fig. 2). Four antennas were installed on the aircraft fuselage and wings with a fixed base length from 3 to 14 m. The SAG mass was 70 kg, and the power consumption was 150 W.

In [78], the authors noted that the architecture with several antennas on the aircraft significantly increased the reliability of information about the accelerations obtained, facilitated the resolution of the phase measurement ambiguity, and provided the generation of additional, in relation to the INS, information about aircraft angles of orientation.

To confirm the performance of the scalar SAG, tests were carried out onboard the Do-128-6 aircraft over a gravimetric test site in Germany in 2003–2004. The error in determining the GDV vertical component was in the range between 3 and 5 mGal and the horizontal components, from 10 to 15 mGal with a spatial resolution of 1 km. The average speed of the aircraft was 70 m/s at an altitude of 300 m above the ground. Each flight began and ended with calibration maneuvers to provide the best observation conditions for estimation of sensor errors. During the survey, the accelerations did not exceed 0.2 m/s^2. At the test site, GA were known with an accuracy of 0.1 mGal and a spatial resolution of 500 m. The maximum GA was 70 mGal [78].

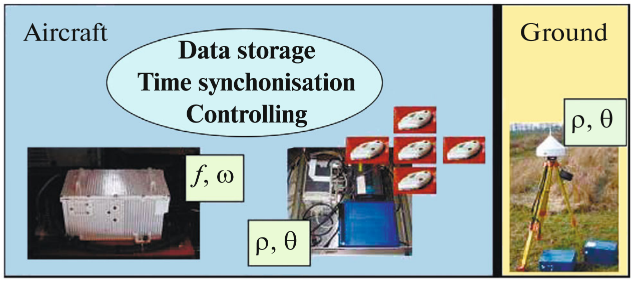

Fig. 2. Component parts of a SAG based on the SAGEM Sigma 30 IMU [78]: f—specific force, ω—angular velocity, ρ—coordinates, θ—aircraft angles of orientation.

3.4. Strapdown Airborne Gravimeter SAGS4, Germany

Strapdown airborne scalar gravimeter SAGS4 (Strapdown Airborne Gravimetry System prototype) was developed at the Bavarian Academy of Sciences and Humanities in 2005. The block diagram of the gravimeter is shown in Fig. 3.

The full acceleration vector was measured with a set of four Q-Flex QA-3000-030 accelerometers with one redundant accelerometer in the vertical channel. The orientation problem was solved using the integrated data generated by a triad of fiber-optic gyroscopes (FOGs) and the multiantenna GPS receiver (MA-GPS).

In the standard configuration of the IMU, shock absorbers (a combination of an elastomer and an air damper) were used for its vibration isolation. The total weight of the SAGS4 was about 30 kg. No in-flight operator service was provided. Adjustment of the thermal control was planned for 2005, following which the SAG was supposed to be calibrated and put into operation. However, after 2006, there has been no mention of the development or operation of the SAGS4 [79].

3.5. Strapdown Airborne Gravimeter SGA-WZ, China

As noted in [80], the first Chinese strapdown airborne scalar gravimeter SGA-WZ was developed in the Laboratory of Inertial Technologies in the National University of Defense Technology (NUDT) in 2008. The SGA-WZ consists of two units (Fig. 4): an IMU and a processing and control unit [81, 82].

As can be seen in Fig. 4, the IMU includes a triad of RLGs (1) and a triad of accelerometers (2) mounted on an antivibration platform. The triads of accelerometers and gyroscopes are spaced apart in order to avoid the impact caused by the RLG dither. Thermal stabilization is carried out by control modules (7) used to regulate the temperature inside the protective thermal shell (6) that covers the inertial sensors.

The processing and control unit consists of a control device (3), uninterruptible power supply (4), and a computer for recording all data and monitoring the status of the operating devices (5). All inertial data are recorded at 2 kHz, while GNSS data from a dual frequency receiver are recorded at 1 or 2 Hz. Tables 3 and 4 show specifications of the gyroscopes and accelerometers [81].

To verify the characteristics of the SGA-WZ gravimeter, laboratory tests were first carried out, which, in particular, showed that the bias of the vertical (Z) accelerometer was 60 mGal over 104 days, the RMSE

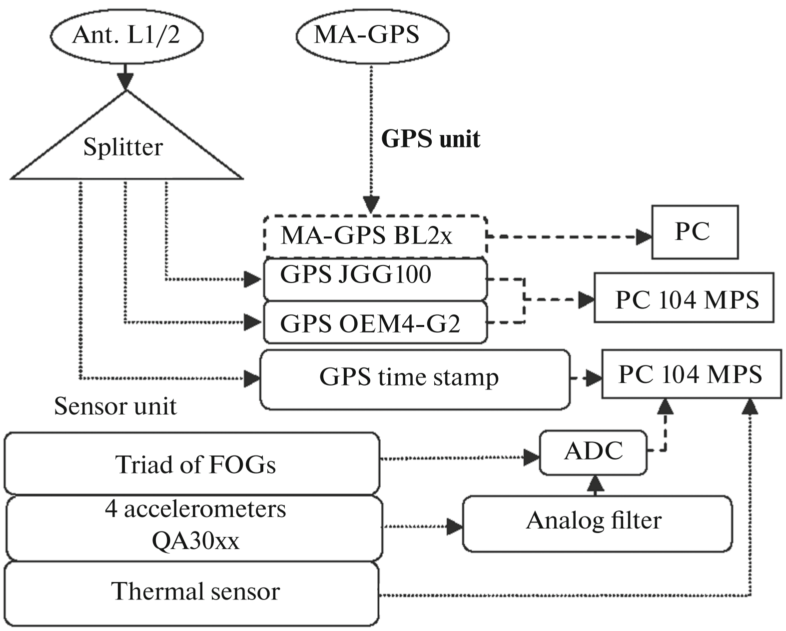

Fig. 3. Block diagram of SAGS4 [79].

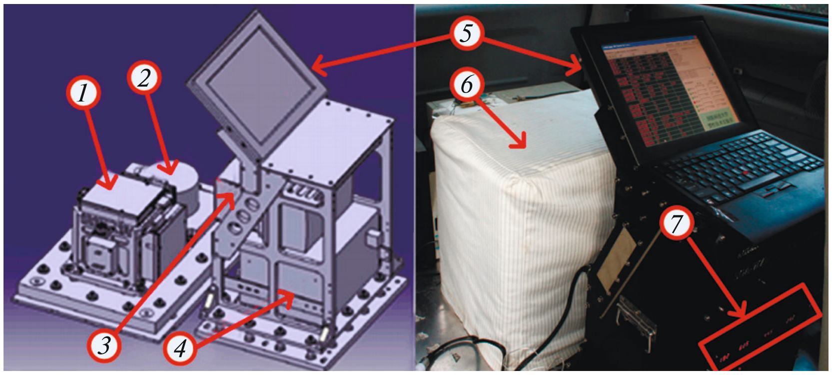

Fig. 4. 3D-model of the SGA-WZ gravimeter without housing (left); external view of the gravimeter (right) [82].

of the readings, taking into account the quadratic model of the bias, varied from 0.3 to 0.6 mGal [81, 83]. Further, road and flight tests were carried out in 2007, 2009, and 2010. Of the in-flight tests, only the latter were successful. They were carried out onboard a Cessna 208 Grand Caravan. The aircraft was controlled by autopilot and the tests were carried out in good weather to minimize the effects of turbulence. The flight altitude was about 400 m, and the average speed was 60 m/s. The test results showed that the RMSE of the GA determination on repeated tacks was 1.6 mGal with a spatial resolution of 4.8 km. The designers noted that the errors in constructing the vertical were not sufficient to determine the horizontal components of the GDV with acceptable accuracy [80].

In 2012, some representatives of the Technical University of Denmark took part in the tests of the SGA-WZ carried out in Greenland in difficult flight conditions over mountains and fiords, with GAs exceeding several hundred mGal, as well as in more favorable conditions over the sea. The flights were carried out at constant altitudes of 2000 m over land and 360 m over sea. The flight speed was about 70 m/s. The results of the GA determination were compared with the data of marine and airborne gravity surveys conducted earlier in this area with LCR gravimeters. The tests showed that the RMSE of the GA determination did not exceed 1 mGal at a spatial resolution of 6 km under conditions of a highly anomalous EGF. However, the long-term stability of the SAG remained the main problem, as it affected the systematic error in determining the GA and depended primarily on the temperature stability of inertial sensors [81, 82].

A three-level thermal control system was developed for the SGA-WZ gravimeter. Each level has its own thermal insulation layer, heating element, temperature sensors, and control unit [84]. The new model of the airborne gravimeter with an improved thermal stabilization system was called SGA-WZ-02. The system is designed as a compact structure (Fig. 5), which greatly reduces its volume and power consumption.

It is noted in [84] that the thermal analysis of the temperature field carried out by means of the ANSYS program made it possible to select new temperature measurement points in the control system, optimize the layout of the heating layer, and choose a new heat-insulating layer. The results of the laboratory and in-flight tests of the SGA-WZ-02 gravimeter together with the gyrostabilized gravimeter GT-2A presented in [84] turned out to be much better than those of the previous gravimeter model: the RMSE in the GA determination was decreased two-fold from 1.5 mGal for SGA-WZ to 0.75 mGal for SGA-WZ-02 at a spatial resolution of 4.8 km.

3.6. Strapdown Airborne Gravimeter GT-X, Russia

The GT-X SAG is based on a 3DOF RLG, four A-17 pendulous accelerometers with horizontal sensitivity axes, and an AK-8 gravity sensor, similar to the one used in gyrostabilized gravimeters of the GT series (Fig. 6). The GT-X gravimeter also includes a thermo-

Table 3. Specifications of the gyroscopes of the SGA-WZ gravimeter

	Bias, °/h		Scale factor	
	instability	repeatability	repeatability (1σ)	nonlinearity (1σ)
X	0.0033	0.00044	8.7×10^{-7}	1.08×10^{-6}
Y	0.0032	0.00038	8.5×10^{-7}	1.07×10^{-6}
Z	0.0029	0.00157	1.1×10^{-6}	1.18×10^{-5}

Table 4. Specifications of the accelerometers of the SGA-WZ gravimeter

Parameter	*X*	*Y*	*Z*
Measurement range, g	±10	±10	±10
Bias, μg	8.1	9.7	2.8
Scale factor stability, ppm	23.3	19.9	5.5
Temperature coefficient, μg/°C	8.4	−3.6	11.5

stat for the accelerometer unit and a shock absorber [85].

The GT-X gravimeter was created by three companies:

• Gravtechology JSK STK, which is responsible for the design and onboard software [71];

• Ramensky Instrument Engineering Plant [88], which developed the software for the RLG and manufactured the prototype gravimeter;

• Laboratory of Control and Navigation of Moscow State University, which developed the gravimeter data postprocessing software [101].

Based on the analysis of numerous airborne gravity survey data obtained with the use of the GT-series gravimeters, the designers formed the requirements for the IMU of the GT-X gravimeter that are presented in Table 5 [85].

The main design features of the GT-X gravimeter are the following. The gravimeter has two pairs of horizontal accelerometers, which made it possible to minimize the error in determining GA caused by the cross-coupling effect and eliminate the problem of spatial displacements of the proof mass. The inertial sensors are attached with a special resonant structure with a counterweight that eliminates the effect of the RLG dither on the gravimeter readings. The survey includes pre-flight and post-flight calibrations of the gravimeter's geometric and instrumental errors, implemented using a special system to provide tilts about three axes. Specifications of the GT-X gravimeter are given in Table 6 [85].

In-flight tests of the GT-X gravimeter prototype were carried out onboard the AN-26 aircraft on four short tacks in steady flight conditions. The measurement accuracy was estimated by comparison with the gyrostabilized GT-2A gravimeter data. The difference in GAs after measurement adjustments was less than 3 mGal. This value can be taken as an estimate of the current accuracy of the GT-X gravimeter [85].

3.7. Series of iMAR Strapdown Airborne Gravimeters, Germany

iMAR Navigation gmbH, Germany, (hereinafter, iMAR) has developed a series of iNAV and iNAT inertial navigation systems (INS) based on quartz accelerometers and gyroscopes of different types—RLG, FOG, and MEMS gyros [86]. They are the basis of these INS and are also used in iMAR SAGs.

iMAR's first scalar SAG was built on the iNAV-RQH-1003 IMU in 2013. The most important functional components of this gravimeter are shown in Fig. 7 [9].

Six Honeywell inertial sensors are combined into an IMU, which, in addition, contains a temperature sensor and a clock. No details about the IMU internal design, in particular, the arrangement of the inertial

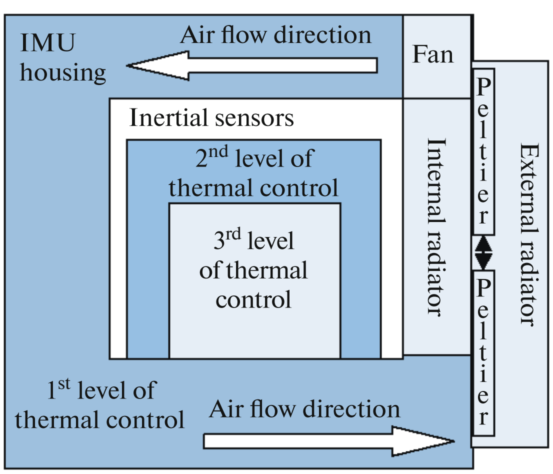

Fig. 5. Structure of the three-level thermal control system of the SGA-WZ-02 gravimeter [84].

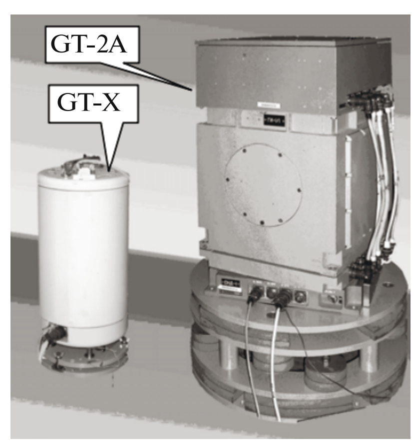

Fig. 6. Strapdown airborne gravimeter GT-X (Russia) [85].

Table 5. Requirements for the IMU of the GT-X gravimeter

Parameter	Value
Horizon calculation (RSME), arcsec	10
LG bias instability, °/h	0.02
Gravimeter scale factor instability	10^{-4}
Gravimeter bias instability, mGal	0.5
Scale factor instability of horizontal accelerometer	5×10^{-4}
Bias instability of horizontal accelerometer, mGal	0.5

Table 6. Specifications of the GT-X gravimeter

Parameter	Value
Dynamic range, g	±1
Power consumption, W	35
Operating temperature, °C	+10...+50
Dimensions, mm	∅240 × 450
Weight, kg	22

sensors and the temperature sensor are available from [9]. The IMU is attached to the housing through shock absorbers, which reduce mechanical shock and high-frequency vibration.

A single-frequency GNSS receiver is used to complement the IMU data with timestamps. The internal transmission of timestamps is a combination of a PPS signal and navigation data in a streaming format that contains information on the date and time.

A miniature board of the PC is used to collect all information, including time-stamped inertial data and real-time navigation solutions. The PC board also allows one to form data on the IMU temperature and data from its temperature sensor. It is noted that the output of the IMU temperature data is of crucial importance for thermal calibrations. Overall dimensions of the iNAV-RQH-1003 IMU are 20 × 20 × 35 cm; weight is 12.5 kg; power consumption is less than 40 W. Characteristics of the inertial sensors are given in Table 7 [9].

In the period from October 2013 to January 2016, five airborne gravity surveys were carried out in different areas with an iNAV-RQH-1003 IMU-based gravimeter. Analysis of the data showed that it was possible to achieve an accuracy of GA determination of the order of 1 mGal or less [9, 87].

In August 2016, the iNAV-RQH-1003 IMU-based SAG was tested aboard a Eurocopter AS350 helicopter in Greenland. That was the first time the SAG was tested onboard a helicopter in a terrain following survey. The RMSE in GA determination was 2 mGal at a spatial resolution of 4.5 km [55].

iMAR SAGs are undergoing continuous development to improve the accuracy and spatial resolution of measurements [86]. According to some authors [9, 89], the main problem SAG designers face is to ensure stability of the accelerometers bias, which, first of all, depends on temperature changes and directly affects the accuracy of determining the GDV components. Various strategies to deal with this problem are considered in literature [48, 90–92], among which are aircraft maneuvers (for example, rotations about the roll or pitch axes); use of repeated or external measurements (for example, discrepancy at tacks crosspoints,

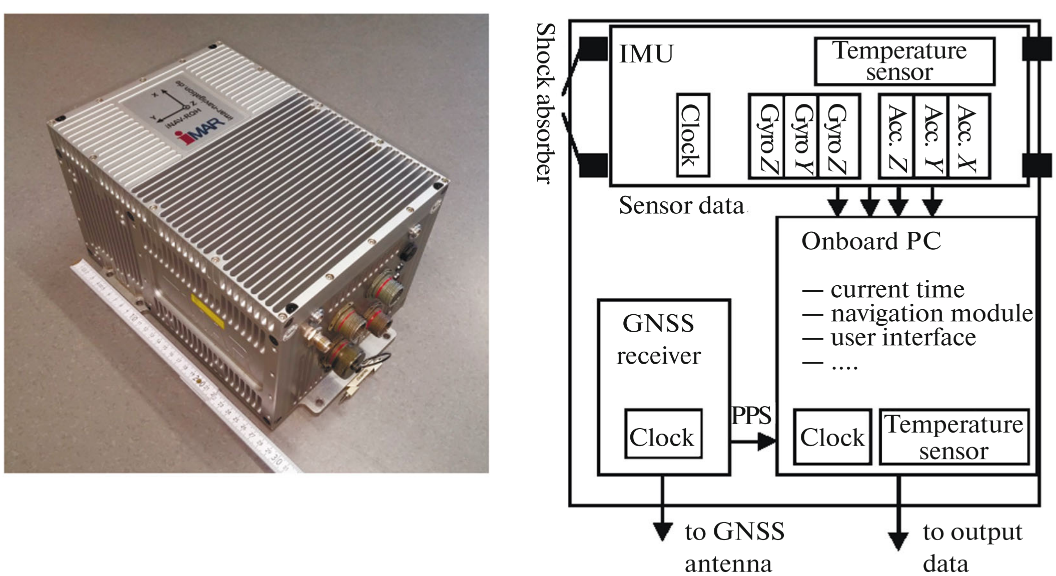

Fig. 7. External view and a diagram of the main parts of the iNAV-RQH-1003 IMU-based gravimeter [9].

Table 7. Characteristics of the iMAR inertial sensors

Parameter	Accelerometers	Gyroscopes
Model	Honeywell Q-Flex QA-2000	Honeywell GG1320A
Type	Quartz pendulous	Ring laser
Measurement range	±20g	±400°/s
Scale factor nonlinearity	<100 ppm	<5 ppm
Bias	<25 μg	<0.003 /h
Random noise	<8 μg/√Hz	<0.002°/√h

global EGF models); special IMU calibration techniques. Each of these strategies has its advantages and drawbacks. As an alternative to thermal calibrations and corrections applied to accelerometers, in [9], it is recommended to use an IMU with an internal thermal stabilization system or a thermally insulated housing for the IMU. iMAR also followed this path and developed the iTempStab temperature stabilization system, which is a heat-insulating housing with built-in Peltier modules. After several hours of warming up, this system stabilizes the iNAT IMU temperature with an error of lower than 0.1°C. The operation algorithm of the iTempStab add-on is described in detail in [89].

In [93] it is noted that although thermal stabilization improves the accuracy of determining the GDV components (especially in the long-wave part of the spectrum), the presence of such a unit raises doubts about the SAG advantages over traditional gyrostabilized gravimeters. An additional temperature stabilization unit increases the SAG dimensions, weight and power consumption. Nevertheless, SAGs of this type are widely used. It is shown that the temperature stabilization unit effectively limits bias of accelerometers and improves estimation of the GDV long-wave component.

The capabilities of the iTempStab thermal stabilization system were studied in the frames of the airborne gravity survey in Turkey in 2017–2018. The RMSE in determining GAs at the cross-points of the tacks was about 3.6 mGal. After the iTempStab unit was installed, it decreased to 0.8 mGal. Comparison with ground survey data showed a decrease in the RMSE in GA determination from 2.19 to 0.94 mGal [89].

It is important to note that gyrostabilized gravimeters still have better long-term stability of readings compared to strapdown gravimeters [93].

One of iMAR's latest developments is the iCORUS-series SAGs, which to a greater extent meet the modern requirements for airborne gravimetric systems (Fig. 8).

There is a low-weight small-sized version of iCORUS SAG, designed for use, for example, in UAVs. It is possible to combine the IMU with an additional unit iDGU-100x, which provides compensation for systematic errors in the GA determination caused by the zero bias of the SAG's inertial sensors. As stated in [94], after removing the linear trend, the measurement error of GA can be decreased from 1.5 to 0.5–0.8 mGal.

Below is a list of the iCORUS series SAGs known to date: iCORUS-01—RLG-based gravimeter; iCORUS-01-wts – gravimeter without thermal stabilization; iCORUS-02—RLG-based gravimeter; iCORUS-02-wts—gravimeter without thermal stabilization; iCORUS-03—FOG-based gravimeter. The

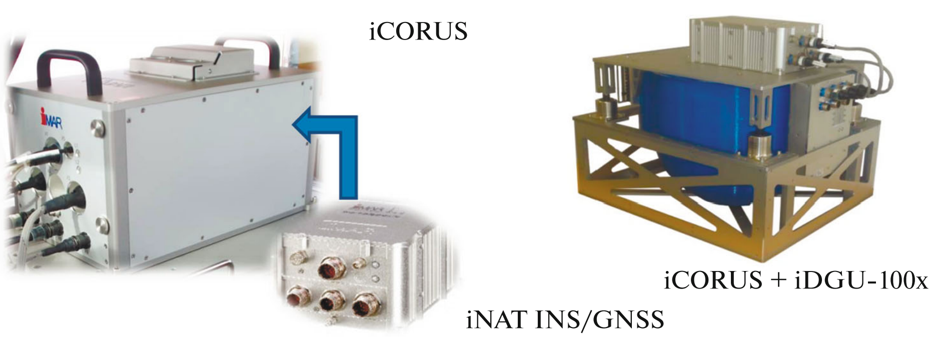

Fig. 8. iCORUS-series SAGs [94].

Table 8. The main characteristics of the inertial sensors.

Sensors	Parameter	IMU		
		iXSea	iNAV-FMS	Litton LN-200
Accelerometers	Random noise, μg/√Hz	15	50	110
	Bias instability, μg	100	1500	1500
Gyroscopes	Random noise, °/h/√Hz	0.09	6.00	9.00
	Bias instability, °/h	0.01	0.75	3.00

Table 9. The results of the SAG comparison

IMU	RSME in gravity anomaly determination, mGal (σ)	Time constant of the filter, s			
		17	60	90	120
iXSea	Repeated tacks	2.1	1.9	1.6	1.5
	Tacks crossings	2.1	2.3	2.5	2.8
	–	–	–	–	–
	Compared with EIGEN-6C4 model	4.4	4.5	4.5	4.5
iNAV-FMS	Repeated tacks	4.3	4.2	4.2	4.1
	Tacks crossings	5.0	4.9	4.8	4.8
	Compared with IXSea IMU data	5.4	5.4	5.5	5.5
	Compared with EIGEN-6C4 model	3.4	3.3	3.0	3.0
Litton LN-200	Repeated tacks	4.8	4.7	4.7	4.6
	Tacks crossings	4.7	4.7	4.8	5.1
	Compared with IXSea IMU data	4.5	4.5	4.5	4.3
	Compared with EIGEN-6C4 model	3.5	3.4	3.1	3.1

first two models of SAGs are subject to export restrictions [94].

3.8. Joint tests of Airborne Gravimeters

This subsection describes some SAGs that are not discussed in detail in the available literature, but are mentioned in the publications devoted to the joint use of different airborne gravimeters.

In 2010, three SAGs were jointly tested over the island of Madeira, Portugal: a SAG with an iMAR iNAV-FMS IMU, a Litton LN-200 IMU-based SAG (subsection 3.2), and an iXSea AIRINS IMU-based SAG, France. The main characteristics of the inertial sensors are shown in Table 8 [48].

The tests were conducted on the ATR 42 aircraft. The airborne gravimeters were placed on a single mounting plate near the aircraft center of mass. The data sampling rate was 100 Hz for the iXSea IMU, 400 Hz for the iNAV-FMS IMU, and 200 Hz for the Litton LN-200 IMU.

The RMSE of the GA determination based on the data of two flights was calculated in four variants:

— for each IMU by comparing the results of measurements on repeated tacks;

— for each IMU by comparing the results of measurements at the crosspoints of the tacks;

— using the results of the higher quality IMU to estimate the accuracy of the two other IMUs;

— for each IMU when compared with the EIGEN-6C4 EGF model reduced to the local topography and survey altitude.

The spatial resolution of the measurements was also analyzed. A low-pass filter with different time constants—17, 60, 90, and 120 s—was used in the post-processing mode.

The results of the accuracy estimation of GA determination are presented in Table 9 [48].

The smallest RSME in GA determination was shown by the iXSea IMU, the RSME of which was 2.1 and 1.6 mGal for repeated tacks and a spatial resolution of 1.7 and 5.0 km, respectively. The iNAV-FMS IMU data processing was difficult because of nonlinear drift in gravimeter readings. However, the results of these tests demonstrated the promise of using the iMAR IMU for strapdown airborne gravimetry. The tactical-grade Litton LN-200 IMU showed an accuracy of about 4.5 mGal at a spatial resolution of 5 km.

4. TRENDS IN THE DEVELOPMENT OF STRAPDOWN INERTIAL AIRBORNE GRAVIMETERS

Current trends in SAG development include the search for ways to develop a currently missing commercially available vector SAG with the required accuracy characteristics. One of the main obstacles to creating such a gravimeter is the error in solving the orientation problem, which, in turn, is determined by the errors of gyroscopic sensors. The orientation error of 1 arcsec is equivalent to the horizontal component error of 5 mGal [36, 37], while the same orientation error for the vertical component is only 5 μGal. In [102, 103], the authors point out that it is possible to achieve an error of determining the horizontal components at a level of 5 mGal by using special methods for processing the results obtained in multiple passes of the survey area.

The designers of airborne gravimeters are working to reduce the weight and dimension characteristics of SAGs in order to use them on a wider class of aircraft, in particular, UAVs, which make it possible to increase the accuracy and resolution of airborne gravity survey owing to the following features:

— low speed and low flight altitude, which form the basis for increasing the spatial resolution of measurements;

— ZUPT corrections, which allow compensation for the errors of the SAG's inertial sensors and improve the accuracy of measurements.

These features provide the competitiveness of airborne gravity survey from UAVs compared to ground-based gravity surveys due to its greater efficiency.

Reference [95] is devoted to the use of SAGs onboard UAVs. Spectral analysis of the IMU and GNSS errors formed the basis to study the influence of the flight speed and dynamics on the accuracy in determining the GDV. Two classes of IMU were considered—navigational and tactical. The paper shows that for the navigation-grade IMU, the low speed of the UAV can be an advantage in the recovery of short wavelengths (<5 km) of the GDV. This is especially significant in determining the GA due to the smaller influence of orientation errors. For tactical-grade IMUs, the low speed of the UAV is a disadvantage, since it limits the recovery of short and medium wavelengths (<30 km) of the anomalous EGF. In terms of flight dynamics, the effect of the phugoid motion was analyzed. It is noted that the low speed of the UAV leads to a short phugoid period compared to heavy aircraft, which is about 13 s. This makes it possible to determine the GDV components with a resolution of less than 1 km. Note that in [96], a technique based on spectral analysis was developed to compare various algorithms for determining GDV components, which makes it possible, among other things, to detect the effect of flight dynamics on the accuracy of their estimation.

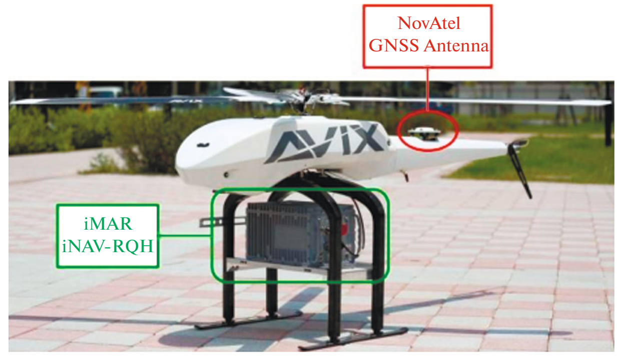

Fig. 9. SAG on an unmanned helicopter [65].

Reference [65] provides information on the creation of a SAG based on the navigation-grade iMAR iNAV-RQH SINS and Novatel GNSS receiver, installed on an unmanned helicopter (Fig. 9), the characteristics of which are presented in Table 10.

Preliminary test results for such UAV showed that the error in determining the GDV components at the crosspoints of the tacks was approximately 4 mGal for the vertical component and 6–11 mGal for the horizontal components with a spatial resolution of 0.5 km. ZUPT correction mode was used to estimate repeatability of the measurement results, which was 2–3 mGal for the GDV vertical component [65].

Reference [97] presents the SAG data processing results obtained by Aerogeofizika Research and Production Company (Russia) [104] during the tests on a UAV BAS-200. The results of measurements during the fourfold passage of the tack are shown in Fig. 10.

Table 10. Characteristics of the unmanned helicopter

Parameter	Value
UAV weight	9 kg
Max takeoff weight	30 kg
Battery weight	5–10 kg
Payload	15 kg
Max operating range	40 km
Max crusing speed	85 km/h
Max autonomy	1 h

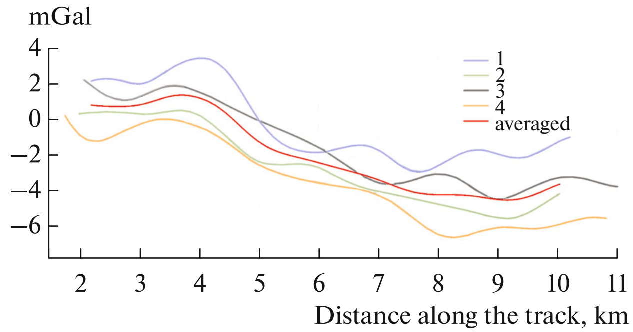

Fig. 10. Results of the gravity anomaly determination on the repeated tack using a UAV BAS-200 [97].

According to the authors, the RMSE of GA determination was ±0.50 mGal.

Another trend in the SAG development is their integration with traditional gyrostabilized gravimeters [98]. On the one hand, this approach deprives strapdown systems of their main advantage; on the other hand, it becomes possible to carry out surveys with increased resolution and high accuracy in difficult turbulent flight conditions, including drape surveys, which is needed in complex airborne geophysical surveys, such as magnetic survey, gamma-ray spectrometry, and electrical survey).

The first attempts at such integration were made by the Danish National Survey and Cadastre Service and the University of Calgary. In June 1998, a joint test of three gravimetric systems—Laseref III strapdown INS/GPS system, the LCR S-type gyrostabilized gravimeter, and the QA 3000 Q-Flex orthogonal triad of accelerometers—was carried out. Reference [74] presents the results and analysis of those tests, compares the measurement techniques and error models of airborne gravimetric systems. It is shown that integration of data from the SAG and the gyrostabilized gravimeter provided a high dynamic range and increased spatial resolution of the survey [34, 73, 98].

Table 11. Characteristics of the iMAR SAG.

Parameter	Value
GA measurement error, mGal	<1.5
Gyro bias, °/h	<0.001
Accelerometer bias, μg	<12
Gyro dynamic range, °/s	±395
Accelerometer dynamic range, g	±20
Power consumption, W	Less than 150
Weight, kg	14

Currently, iMAR is conducting research in this area. Airborne gravimeters of the iCORUS family are designed in a lightweight version to be used on UAVs, with a view of joint operation with an iDGU-100x unit to increase the measurement accuracy [94].

In October—November 2020, Aerogeofizika conducted an airborne gravity survey onboard a Cessna 208B aircraft using two gravimeters: a Gravtekhnologiya GT-3 gyrostabilized gravimeter and an iMAR strapdown gravimeter, the characteristics of which are given in Table 11 [99].

The airborne gravity survey included 48 tacks with a total length of 12700 km and was carried out during 12 flights. The average flight speed was 70 m/s, and the altitude relative to the WGS84 ellipsoid was 680 m. As a result of the survey data processing, it was noted that in general, the GAs obtained by two gravimeters were similar, and the main differences concerned the highest frequency components of the GA. The RSME in GA determination was about 0.9 mGal for the two types of gravimeters.

The next stage of work conducted by Aerogeofizika was the use of SAG in terrain following surveys. In 2021, this mode was used in the work complemented with airborne gravity survey [97]. Flight speed varied within 150—180 km/h, duration, up to 6 hours. The total flight altitude range on the survey lines, dictated by the terrain height, was about 900 m, and the range of the SAG-recorded accelerations was 2300 Gal with a standard deviation on the survey lines of ±153 Gal. The RMSE in the GA determination, estimated by the intrinsic convergence, was ±0.52 mGal [100]. In general, the results of the surveys have shown that the integration of SAG into the airborne geophysical system, which is capable of performing high-precision measurements in terrain following surveys, significantly increases the reliability of data interpretation and the geological efficiency of airborne geophysical work without a significant increase in the cost of surveying [99, 100].

CONCLUSIONS

1. The development of technical means capable of providing a solution to the problems of airborne gravimetry at a new technical and economic level based on the latest achievements in the field of strapdown and satellite navigation systems, electronics, informatics, and computer technology is relevant and promising.

2. Strapdown inertial gravimetric systems and SINS integrated with GNSS are practically identical with respect to the hardware composition. The differences are only in the requirements to the accuracy of inertial sensors, the EGF knowledge, the composition and accuracy GNSS equipment. These systems are certainly different in the set of output data, which is

dictated by the different purposes of these systems. At the same time, it seems appropriate to create a system which will be able to perform the functions of both systems, depending on a particular application. In the authors' opinion, there is a trend like that.

3. The absence of stabilization systems in strapdown gravimeters allows reducing their cost, power consumption, weight and overall dimensions, which opens up possibilities for their application on a wider range of aircraft, in particular, UAVs. The use of UAVs provides a flexible system of gravity survey, which has increased accuracy and detail, and also makes it possible to perform measurements in terrain following survey.

4. Vector gravimeters have important advantages over scalar ones, since they create the prerequisites to determine DOV, geoid heights, and second derivatives of the geopotential directly from their readings, which, in turn, make it possible to detect drastic changes in the structure of the gravitational field.

5. Zero bias of accelerometers is the dominant source of errors in determining GDV components. Various strategies are being developed to deal with this problem: aircraft maneuvers, elimination of linear trends of zero bias using repeated or external measurements. The most important task of reducing zero bias is to develop accurate means of thermal control and thermal stabilization. With this aim in view, it is necessary to search for a compromise in order to achieve high stabilization accuracy with minimal increase in the dimensions and power consumption of the gravimeter.

6. The error of gyroscopic sensors additionally limits the accuracy of determining the GDV horizontal components. The orientation error of 1 arcsec is equivalent to the 5 mGal error in determining the horizontal components. Estimates for determining the GDV horizontal components vary widely, with the most optimistic ones being 5–10 mGal. At the same time, the achievement of such accuracy is only possible with the implementation of special methods for processing the data obtained with multiple passes of the survey area.

7. A separate problem is obtaining reference values of gravity anomaly along the flight trajectory in the course of SAG tests. In this connection, it is necessary to carefully choose the test site (anomality and knowledge gravity field) as well as the time of testing day (to minimize turbulence and atmospheric effects on GNSS signals).

8. Many countries, such as the USA, Canada, Germany, China, Denmark, Portugal, and Russia invest heavily in the development of airborne gravimetry and SAGs, in particular. At present, the leading position on the SAG market belongs to iMAR, Germany, which manufactures not only a series of IMUs that can be used as a basis for SAGs, but also of iCORUS SAGs that meet up-to-date requirements for measuring gravity from aircraft.

9. iCORUS-series SAGs provide the error of gravity anomaly determination less than 1.5 mGal with gyroscopic sensors having the drift rate of no worse than 0.003°/h, random noise, no worse than $0.002°/\sqrt{h}$, and accelerometers with zero bias less than 25 μg and random noise less than 8 μg/Hz. When integrated with the iDGU-100x unit, the error of the gravity anomaly becomes less than 1 mGal. There is a version of low-weight and small-sized iCORUS gravimeter intended to be used onboard UAVs.

ACKNOWLEDGMENTS

We thank A.A. Golovan and Yu.A. Litmanovich for their valuable comments during the revision of the paper, which allowed us to significantly improve it.

FUNDING

This work was supported by the Russian Scientific Foundation, project no. 18-19-00627, https://rscf.ru/project/18-19-00627.

CONFLICT OF INTEREST

The authors declare that they have no conflicts of interest.

REFERENCES

1. Shimbirev, B.P., *Teoriya figury Zemli* (Theory of the Earth's Figure), Moscow: Nedra, 1975.
2. Ogorodova, L.V., Shimbirev, B.P., and Yuzefovich, A.P., *Gravimetriya* (Gravimetry), Moscow: Nedra, 1978.
3. Dehlinger, P., *Marine Gravity*, Elsevier, 1978.
4. Panteleev, V.L., *Osnovy morskoi gravimetrii* (Fundamentals of Marine Gravimetry), Moscow: Nedra, 1983.
5. Torge, W., *Gravimetry*, Berlin: de Gruyter, 1989.
6. Seeber, G., *Satellite Geodesy: Foundations, Methods and Applications,* Berlin: de Gruyter, 2003, second edition. https://doi.org/10.1515/9783110200089
7. Hofmann-Wellenhof, B. and Moritz, H., *Physical Geodesy,* Springer, 2006.
8. *Gravimetriya i geodeziya* (Gravimetry and Geodesy), Brovar, B.V., Ed., Moscow: Nauchnyi mir, 2010.
9. Becker, D., Advanced Calibration Methods for Strapdown Airborne Gravimetry, *PhD thesis*, Technische Universität Darmstadt, 2016.
10. *Methods and Technologies for Measuring the Earth's Gravity Field Parameters,* Peshekhonov, V.G. and Stepanov, O.A., Eds., Springer, 2022. https://doi.org/10.1007/978-3-031-11158-7
11. Jensen, T.E., *Airborne Strapdown Gravity Measurements for Geodesy and Geophysics*, Technical University of Denmark, 2018.
12. Molev, V.P., *Metodika i tekhnika nazemnoi gravimetricheskoi s"emki* (Methods and Facilities for the

Ground Gravity survey), Vladivostok: Far Eastern Federal University, 2019.

13. Koneshov, V.N., Mikhailov, P.S., Solov'ev, V.N., and Zheleznyak, L.K., Modern global models of the Earth's gravity field in the World Ocean: Accuracy estimates and application prospects, *33-ya konferentsiya pamyati N.N. Ostryakova* (33rd Conference in Memory of N.N. Ostryakov), St. Petersburg: Elektropribor, 2022.
14. *GOST* (State Standard) *24284-80: Gravimetric and Magnetic Exploration. Terms and definitions*, 1980.
15. Bolotin, Yu.V. and Golovan, A.A., Methods of inertial gravimetry, *Moscow University Mechanics Bulletin*, 2013, vol. 68, no. 5, pp. 117–125.
16. Schwarz, K.P., Inertial surveying and geodesy, *Reviews of Geophysics*, 1983, vol. 21, no. 4, pp. 878-890.
17. Wei, M. and Schwarz, K.P., Flight test results from a strapdown airborne gravity system, *Journal of Geodesy*, 1998, vol. 72, no. 6, pp. 323–332.
18. Panteleev, V.L., Problems in inertial gravimetry, *Izvestia vuzov. Geologiya i razvedka*, 1997, no. 26, pp. 113–122.
19. Panteleev, V.L. and Levitskaya, Z.N., Major problems in inertial vector gravimetry, *Izvestiya vuzov. Geodeziya i aerofotos"emka*, 2000, no. 1, pp. 77–91.
20. Panteleev, V.L., *Fil'tratsiya v zadachakh inertsial'noi gravimetrii* (Filtering in Inertial Gravimetry), LAP LAMBERT Academic Publishing, 2012.
21. Kwon, J.H., *Airborne vector gravimetry using GPS/INS*, Report No.453, The Ohio State University, Columbus, Ohio 43210–1275, April 2000.
22. Tyuvin, A.V., Afonin, A.A., and Sulakov, A.S., Using functionally redundant accelerometer units in strapdown navigation gravimetric systems, *Trudy MAI*, 2016, no. 91.
23. Schwarz, K.P., Geoid profiles from an integration of GPS satellite and inertial data, *Bolletino di Geodesia e Scienze Affini*, Anno XLVI, 1987, no. 2, pp. 117–131.
24. Jekeli, C. and Kwon, J.H., Results of airborne vector (3-D) gravimetry, *Geophysical Research Letters*, 1999, vol. 26, no. 23, pp. 3533–3536.
25. Jekeli, C. and Kwon, J., Geoid profile determination by direct integration of GPS/INS vector gravimetry, *Journal of Geophysical Research*, 2002, vol. 107, no. B10. https://doi.org/101029/2001JBod626
26. Vasco, D.W., Resolution and variance operators of gravity and gravity gradiometry, *Geophysics*, 1989, vol. 54, no. 7, pp. 889–899.
27. Pawlowski, R. Gravity gradiometry in resource exploration, *The Leading Edge*, 1998, vol. 17, no. 1, pp. 51–52.
28. Jekeli, C., A review of gravity gradiometer survey system data analysis, *Geophysics*, 1993, vol. 58, no. 4, pp. 508–514.
29. Zlotnikov, D., Superior detective work: The promise of airborne gravity gradiometry. *Earth Explorer, Energy Report*, June 2011, pp. 5–7.
30. Evstifeev, M.I., The state of the art in the development of onboard gravity gradiometers, *Gyroscopy and Navigation,* 2017, vol. 8, no. 1, pp. 68–79. https://doi.org/10.1134/S2075108717010047
31. Dzhilavdari, I.Z. and Riznookaya, N.N., Development steps and state of the art in onboard gravity gradiometers, *Pribory i metody izmerenii*, 2016, vol. 7, no. 3, pp. 235–246.
32. Jekeli, C., Theoretical fundamentals of airborne gradiometry, *Airborne Gravity for Geodesy Summer School*, 23–27 May 2016.
33. Veryaskin, A.V. *Gravity, Magnetic and Electromagnetic Gradiometry*, IOP Publishing Ltd, 2021, second edition.
34. Hein, G.W., Progress in airborne gravimetry: Solved, open and critical problems, *Proceedings of the IAG Symposium on Airborne Gravity Field Determination, IUGG XXI General Assembly*, Boulder, Colorado, USA, July 2–14 1995, pp. 3–11.
35. Kwon, J.H. and Jekeli, C., A new approach for airborne vector gravimetry using GPS/INS, *Journal of Geodesy,* 2001, vol. 74, pp. 690–700. https://doi.org/10.1007/s001900000130
36. Hannah, J., *Airborne gravimetry: A status report*, Prepared for the Surveyor General Land Information New Zealand, Otago University, New Zealand, 2001.
37. Bolotin, Yu.V., Golovan, A.A., and Parusnikov, N.A., *Uravneniya aerogravimetrii. Algoritmy i rezul'taty ispytanii* (Airborne Gravimetry Equations. Test Algorithms and Results), Moscow: Moscow State University, 2002.
38. Harlan, R.B., Eotvos corrections for airborne gravimetry, *Journal of Geophysical Research*, 1968, vol. 73, pp. 4675–4679. https://doi.org/10.1029/JB073i014p04675
39. Groves, P.D., *Principles of GNSS, Inertial and Multisensor Integrated Navigation Systems*, Boston, London: Artech House, 2013, second edition.
40. Selivanova, L.M. and Shevtsova, E.V., *Intertsial'nye navigatsionnye sistemy*. (Inertial navigation systems), Part 1, *Odnokanal'nye intertsial'nye navigatsionnye sistemy* (Single-channel inertial navigation systems), Moscow: Bauman Moscow State Technical University, 2012.
41. Johann, F., Becker, D., Becker, M., Forsberg, R., and Kadir, M. The direct method in strapdown airborne gravimetry – A Review, *Zeitschrift für Geodäsie, Geoinformation und Landmanagement*, 2019, vol. 144, no. 5. https://doi.org/10.12902/zfv-0263-2019
42. Andreev, V.D., *Teoriya inertsial'noi navigatsii. Avtonomnye sistemy* (Theory of Inertial Navigation. Autonomous Systems), Moscow: Nauka, 1966.
43. Britting, K.R., *Inertial navigation systems analysis*, New York: Wiley &Sons, 1971.
44. Emel'yantsev, G.I. and Stepanov, A.P., *Integrirovannye inertsial'no-sputnikovye sistemy orientatsii i navigatsii* (Integrated INS/GNSS Orientation and Navigation Systems), St. Petersburg: Concern CSRI Elektropribor, 2016.
45. Ishlinskii, A. Yu., *Orientatsiya, giroskopy, inertsial'naya navigatsiya* (Attitude Determination, Gyroscopes, and Inertial Navigation), Moscow: Nauka, 1976.
46. Johann, F., Becker, D., Becker, M., and Ince, E.S., Multi-scenario evaluation of the direct method in strapdown airborne and shipborne gravimetry, in: *International Association of Geodesy Symposia*, 2020,

Springer, Berlin, Heidelberg, https://doi.org/10.1007/1345_2020_127

47. Jekeli, C. and Garcia, R., GPS phase accelerations for moving-base vector gravimetry, *Journal of Geodesy*, 1997, vol. 71, pp. 630–639. https://doi.org/10.1007/s001900050130
48. Ayres-Sampaio, D., Deurloo, R., Bos, M., Magalhaes, A., and Bastos, L., A comparison between three IMUs for strapdown airborne gravimetry, *Surveys in Geophysics*, 2015, vol. 36, no. 4, pp. 571–586. https://doi.org/10.1007/s10712-015-9323-5
49. Bruton, A.M. and Schwarz, K.P., Airborne gravity estimation using adaptive filters, In *Proceedings of International Symposium on Kinematic Systems in Geodesy, Geomatics and Navigation* (KIS97), Banff, Canada, June 3–6, 1997, pp. 605-612.
50. Jekeli, C., *Inertial Navigation Systems with Geodetic Applications*, Berlin: De Gruyter, 2001. https://doi.org/10.1515/9783110800234
51. Stepanov, O.A., *Osnovy teorii otsenivaniya s prilozheniyami k zadacham obrabotki navigatsionnoi informatsii* (Fundamentals of the Estimation Theory with Applications to the Problems of Navigation Information Processing), Part 1, *Vvedenie v teoriyu otsenivaniya* (Introduction to the Estimation Theory), St. Petersburg: Concern CSRI Elektropribor, 2009, ISBN 978-5-900780-86-3.
52. Stepanov, O.A., Optimal and suboptimal filtering in integrated navigation systems, in *Aerospace Navigation Systems*, Nebylov, A. and Watson, J., Eds., John Wiley & Sons Ltd., 2016, pp. 244–298.
53. Stepanov, O.A., Koshaev, D.A., and Motorin, A.V., Identification of gravity anomaly model parameters in airborne gravimetry problems using nonlinear filtering methods, *Gyroscopy and Navigation*, 2015, vol. 6, no. 4, pp. 318–323. https://doi.org/10.1134/S2075108715040136
54. Motorin, A.V., Koshaev, D.A., and Stepanov, O.A., Performance analysis of the use of satellite measurements in marine gravimetry, *26th St. Petersburg International Conference on Integrated Navigation Systems*, St. Petersburg: Elektropribor, 2019, pp. 282–287.
55. Jensen, T.E. and Forsberg, R., Helicopter test of a strapdown airborne gravimetry system, *Sensors*, 2018, no. 18, no. 9, 3121. https://doi.org/10.3390/s18093121
56. Thompson, L.G.D., Airborne gravity meter test, *Journal of Geophysical Research*, 1959, vol. 64, no. 4, ISSN: 01480227. https://doi.org/10.1029/JZ064i004p00488
57. Thompson, L.G.D. and LaCoste, L.J.B., Aerial gravity measurements, *Journal of Geophysical Research*, 1960, vol. 65, no. 1, pp. 305–322. ISSN: 01480227. https://doi.org/10.1029/JZ065i001p00305
58. Brozena, J.M., Mader, G.L., and Peters, M.F., Interferometric Global Positioning System: Three-dimensional positioning source for airborne gravimetry, *Journal of Geophysical Research*, 1989, vol. 94, no. B9, pp. 153–162. https://doi.org/10.1029/JB094iB09p12153
59. Schwarz, K.R, Cannon, M.E., and Wong, R.V.C., A comparison of GPS kinematic models for the determination of position and velocity along a trajectory, *Manuscripta Geodetica*, 1989, vol. 14, pp. 345–353.
60. Kleusberg, A., Peyton, D., and Wells, D., Airborne gravimetry and the Global Positioning System, *IEEE Symposium on Position Location and Navigation. A Decade of Excellence in the Navigation Sciences*, IEEE, 1990, pp. 273–278. https://doi.org/10.1109/PLANS.1990.66188
61. Forsberg, R., Vassiliou, A., Schwarz, K., and Wong, R., Inertial gravimetry - Comparison of Kalman filtering-smoothing and post-mission adjustment techniques, *Bulletin geodesique*, 1986, vol. 60, no. 2, pp. 129–142. https://doi.org/10.1007/BF02521013
62. Dmitriev, S.P., *Inertsial'nye metody v inzhenernoi geodezii* (Inertial Methods in Engineering Geodesy), St. Petersburg: CSRI Elektropribor, 1997, ISBN 5-900780-07-4.
63. Lobusov, E.S. and Fomichev, A.V., A study of ZUPT mode for strapdown inertial navigation system of a ground vehicle, *Vestnik MGTU im. Baumana*, Series *Priborostroenie*, 2014, no. 6, pp. 15–24.
64. Glennie, C. and Schwarz, K.P., Airborne gravity by strapdown INS/DGPS in a 100 km by 100 km area of the rocky mountains, *Proceedings of International Symposium on Kinematic Systems in Geodesy, Geomatics and Navigation* (KIS97), Banff, Canada, June 3-6, 1997, pp. 619–624.
65. Lin, C.A., Chiang, K., Dongkai, Dai W., and Kuo, C.Y., Integration of INS and GNSS for gravimetric application with UAS, *ISPRS TC I Mid-term Symposium "Innovative Sensing – From Sensors to Methods and Applications"*, 10–12 October 2018, Karlsruhe, Germany.
66. Honeywell https://www.honeywell.com/us/en.
67. Northrop Grumman https://www.northropgrumman.com.
68. SAFRAN https://www.safran-group.com.
69. iXSea https://www.ixsea.com.
70. iMAR https://www.imar-navigation.de.
71. Gravtechology, JSK STC https://www.ooo-npt-gravtekhnologia.
72. Bruton, A., Improving the accuracy and resolution of SINS/DPGS airborne gravimetry, *PhD thesis*, The University of Calgary, 2000.
73. Glennie, C.L., Schwarz, K.P., Bruton A.M., Forsberg, R., Olesen, A.V., and Keller, K., A comparison of stable platform and strapdown airborne gravity, *Journal of Geodesy*, 2000, vol. 74, no. 5, pp. 383–389. https://doi.org/10.1007/s001900000082
74. Glennie, C.L., An analysis of airborne gravity by strapdown INS/DGPS, *PhD thesis*, Department of Geomatics Engineering, The University of Calgary, 1999, UCGE Report No. 20125.
75. Bruton, A., Hammada, Y., Ferguson, S., Schwarz, K., Wei, M., and Halpenny, J., A comparison of inertial platform, damped 2-axis platform and strapdown airborne gravimeter, *Proceedings of the International Symposium on Kinematic Systems in Geodesy, Geomatics and Navigation,* Banff, Canada, 2001, pp. 542–550.
76. Tomé, P., Integration of inertial and satellite navigation systems for aircraft attitude determination, *PhD thesis*, Faculty of Sciences of the University of Porto, 2002.

77. Bastos, L., Tome´, P., Cunha, T., Fernandes, M.J., and Cunha, S., Gravity anomalies from airborne measurements: Experiments using a low cost IMU device, in *Gravity, Geoid and Geodynamics*, Sideris, M., Ed., 2000, International Association of Geodesy Symposia, vol. 123, Springer, Berlin, 2002, pp. 253–258. https://doi.org/10.1007/978-3-662-04827-6_42

78. Kreye, Ch., Hein, G.W, and Zimmermann, B., Evaluation of airborne vector gravimetry using GNSS and SDINS observations, in *Observation of the Earth System from Space,* Flury, J., Rummel, R., Reigber, C., Rothacher, M., Boedecker, G., and Schreiber, U., Eds., Berlin/Heidelberg: Springer, 2006, pp. 447–461. https://doi.org/10.1007/3-540-29522-4_29

79. Boedecker, G. and Stiirze, A., SAGS4 – Strapdown airborne gravimetry system analysis, in *Observation of the Earth System from Space*, Flury, J., Rummel, R., Reigber, C., Rothacher, M., Boedecker, G., and Schreiber, U., Eds., Berlin/Heidelberg: Springer, 2006, pp. 463–478. https://doi.org/10.1007/3-540-29522-4_30

80. Cai, S., Wu, M., Zhang, K., Cao, J., Tuo, Z., and Huang, Y., The first airborne scalar gravimetry system based on SINS/DGPS in China, *Science China Earth Sciences*, December 2013, vol. 56, no. 12, pp. 2198–2208. https://doi.org/10.1007/s11430-013-4726-y

81. Huang, Y., Olesen, A.V., Wu, M., and Zhang, K., SGA-WZ: A new strapdown airborne gravimeter, *Sensors*, 2012, vol. 12, no. 7, pp. 9336–9348, https://doi.org/10.3390/s120709336

82. Zhao, L., Forsberg, R., Wu, M., Olesen, A.V., Zhang, K., and Cao, J., A flight test of the strapdown airborne gravimeter SGA-WZ in Greenland, *Sensors*, 2015, vol. 6, pp. 13258–13269. https://doi.org/10.3390/s150613258

83. Cai, S., Zhang, K., Wu, M., and Huang, Y., Long-term stability of the SGA-WZ strapdown airborne gravimeter, *Sensors*, 2012, vol. 12, no. 8, pp. 11091–11099. https://doi.org/10.3390/s120811091

84. Cao, J., Wang, M., Cai, S., Zhang, K., Cong, D., and Wu, M., Optimized design of the SGA-WZ strapdown airborne gravimeter temperature control system, *Sensors,* 2015, vol. 15, no. 12, pp. 29984-29996. https://doi.org/10.3390/s151229781

85. Berzhitskii, V.N., Ermakov, M.A., Ilyin, V.N., Smoller, Yu.L., Yurist, S.Sh., Bolotin, Yu.V., Golovan, A.A., Parusnikov, N.A., Gavrov, E.V., Rekunov, D.A., Fedorov, A.E., Gabell, B., Tuckett, H., Olson, D., and Shabanov, A.V., Airborne strapdown gravimeter GT-X, *IAG Symposium on Terrestrial Gravimetry "Static and Mobile Measurements",* St. Petersburg: Elektropribor, 2010.

86. Hoss, M., Dreyer, A, von Hinueber, E.L., Urli, R., and Lapeyrade, F., Innovative inertial measurement data acquisition and processing for aircraft surveying up to airborne gravimetry, *The European Test and Telemetry Conference* – ETTC 2020. https://doi.org/10.5162/ettc2020/1.3

87. Becker, D., Becker, M., Olesen, A.V., Nielsen, J.E., and Forsberg, R., Latest results in strapdown airborne gravimetry using an iMAR RQH unit, *4th IAG Symposium on Terrestrial Gravimetry,* St. Petersburg: Elektropribor, 2016, pp. 19–25.

88. Ramensky Instrument Engineering Plant https://rpz.kret.tech

89. Simav, M., Becker, D., Yildiz, H., and Hoss, M., Impact of temperature stabilization on the strapdown airborne gravimetry: A case study in Central Turkey, *Journal of Geodesy*, 2020, vol. 94, no. 4, 41. https://doi.org/10.1007/s00190-020-01369-5

90. Glennie, C.L. and Schwarz, K.P., A comparison and analysis of airborne gravimetry results from two strapdown inertial/DGPS systems, *Journal of Geodesy,* 1999, vol. 73, no. 6, pp. 311–321. https://doi.org/10.1007/s001900050248

91. Hwang, C., Hsiao, Y.S., and Shih, H.C., Data reduction in scalar airborne gravimetry: Theory, software and case study in Taiwan, *Computers & Geosciences*, 2006, vol. 32, no. 10, pp. 1573-1584. https://doi.org/10.1016/j.cageo.2006.02.015

92. Deurloo, R., Development of a Kalman filter integrating system and measurement models for a low-cost strapdown airborne gravimetry system, *PhD thesis*, Faculty of Sciences of the University of Porto, 2011.

93. Jensen, T.E., Olesen, A.V., Forsberg, R., Olsson, P.-A., and Josefsson, Ö., New results from strapdown airborne gravimetry using temperature stabilization, *Remote Sensing*, 2019, vol. 11, no. 22, 2682. https://doi.org/10.3390/rs11222682

94. iCORUS https://imar-navigation.de/downloads/iCORUS.pdf.

95. Deurloo, R., Bastos, L., and Bos, M. On the use of UAVs for strapdown airborne gravimetry, in *Geodesy for Planet Earth*, Kenyon, S., Pacino, M.C., and Marti, U., Eds., 2012, International Association of Geodesy Symposia, vol. 136. Springer, Berlin, pp. 255–261. https://doi.org/10.1007/978-3-642-20338-1_31

96. Bolotin, Yu.V. and Vyazmin, V.S., Spectral analysis of the airborne vector gravimetry problem, *Journal of Mathematical Sciences*, 2021, vol. 253, no. 6, pp. 778–795. https://doi.org/10.1007/s10958-021-05269-7

97. Vyazmin, V.S., Golovan, A.A., Bolotin, Yu.V., Brovkin, G.I., and Kontarovich, O.R., Technologies and results of strapdown airborne gravimeter data processing in areal surveys with different aircraft, *33-ya konferentsiya pamyati N.N. Ostryakova* (33rd Conference in Memory of N.N. Ostryakov), St. Petersburg: Elektropribor, 2022, pp. 157–160.

98. Jensen, T.E., Nielsen, J.E., Olesen, A.V., and Forsberg, R., Strapdown airborne gravimetry using a combination of commercial software and stable-platform gravity estimates, Springer International Publishing AG 2017, Vergos, G.S. et al., Eds., *International Symposium on Gravity, Geoid and Height Systems 2016*, International Association of Geodesy Symposia 148. https://doi.org/10.1007/1345_2017_9

99. Brovkin, G.I., Kontarovich, O.R., Golovan, A.A., and Vyazmin, V.S., Results of the first in Russia airborne gravity survey with a strapdown gravimeter, *Proceedings of the 4th International Geological Geophysical Conference and Exhibition GeoEurasia-2021*, vol. 2, Tver: Polipress, 2021.

100. Babayants, P.S., Brovkin, G.I., Kontarovich, O.R., Vyazmin, V.S., and Golovan, A.A., Features of modern airborne gravity surveys, *33-ya konferentsiya pamyati N.N. Ostryakova* (33rd Conference in Memory of N.N. Ostryakov), St. Petersburg: Elektropribor, 2022.

101. Control and Navigation Laboratory at Moscow State University http://NavLab.ru

102. Senobari, M.S., New results in airborne vector gravimetry using strapdown INS/DGPS, *Journal of Geodesy*, 2010, vol. 84, pp. 277–291. https://doi.org/10.1007/s00190-010-0366-6

103. Vyazmin, V.S., Golovan, A.A., and Bolotin, Yu.V., New strapdown airborne gravimetry algorithms: Testing with real flight data, *28th St. Petersburg International Conference on Integrated Navigation Systems*, St. Petersburg: Elektropribor, 2021, ISBN 978-5-91995-081-3.

104. Aerogeofizika Research and Production Company https://www.aerogeo.ru